SIAM J. NUMER. ANAL.
Vol. 58, No. 5, pp. 3068–3090

APPROXIMATE DECONVOLUTION WITH CORRECTION: A MEMBER OF A NEW CLASS OF MODELS FOR HIGH REYNOLDS NUMBER FLOWS*

ALEXANDER E. LABOVSKY†

Abstract. We propose a new family of models for fluid flows at high Reynolds numbers, large eddy simulation with correction (LES-C), that combines a LES approach to turbulence modeling with a defect correction methodology. We investigate, both numerically and theoretically, one of these models, based on the approximate deconvolution model (ADM). The new model, approximate deconvolution with correction, is shown to be stable and higher order accurate with respect to the filtering width. It is shown to outperform its most natural competitor, the ADM, on a variety of benchmark problems. These include the computation of errors (on a problem with known solution), a benchmark problem of finding maximal drag and lift coefficients, flow past the step, and the discussion on Taylor–Green vortex solutions.

Key words. defect correction, turbulence model, large eddy simulation, approximate deconvolution

AMS subject classifications. 65M12, 76D05, 76F65

DOI. 10.1137/20M1311600

1. Introduction.

We propose to use defect correction for modeling incompressible turbulent flows.

Consider the Navier–Stokes equations (NSEs) for an incompressible fluid flow in $\Omega \in \mathbb{R}^d$: find the velocity-pressure pair $u : \Omega \times [0,T] \to \mathbb{R}^d (d = 2,3)$ and $p : \Omega \times (0,T] \to \mathbb{R}$ satisfying

$$\begin{aligned} &u_t + u \cdot \nabla u - \nu \Delta u + \nabla p = f, \text{ for } x \in \Omega, 0 < t \le T, \\ &\nabla \cdot u = 0, \ x \in \Omega, \text{ for } 0 \le t \le T, \\ &u(x,0) = u_0(x), \text{ for } x \in \Omega, \end{aligned} \tag{1.1}$$

with zero (no-slip) boundary conditions for velocity and the normalization condition $\int_\Omega p(x,t)\, dx = 0$ for pressure, $0 < t \le T$.

The defect correction methods have been known for more than 50 years, and yet they have never been popular in the CFD community. The defect correction idea has been used as a regularization technique, e.g., [35, 19, 18, 30]; the author used it to replace turbulence modeling in [28], relatively unsuccessfully. In recent years, with the development of the so-called deferred correction methods (defect correction idea, applied to temporal discretizations [17, 43, 44, 11]), successful "marriage" of deferred correction and (incompressible) turbulence modeling has improved the temporal accuracy of turbulence models [23]. However, defect correction methods are still considered too crude to be helpful in modeling flows at high Reynolds numbers. The two main reasons are the increased computational time and the well-known "asymptotic convergence" feature of any defect correction method: the theoretically claimed convergence rates are only seen in numerical testing after several steps of spatial mesh

*Received by the editors January 8, 2020; accepted for publication (in revised form) August 24, 2020; published electronically October 27, 2020.
https://doi.org/10.1137/20M1311600
†Department of Mathematical Sciences, Michigan Technological University, Houghton, MI 49931 USA (aelabovs@mtu.edu).

refinement. This last issue is the main drawback in the eyes of a turbulence model developer, as the computations become prohibitively expensive when the spatial mesh diameter gets too small.

In this paper, we introduce a way of combining the defect correction approach and turbulence modeling, so that both of the above issues are resolved. We will demonstrate that adding a correction step to an existing turbulence model (therefore, treating the model itself as a "defect") allows us to achieve the predefined tolerance in less than half the time that would have been needed for the underlying turbulence model to achieve this tolerance. In other words, instead of taking longer to create an approximate solution of desired accuracy, the proposed models will do it twice as fast as the existing turbulence models—see the discussion in section 4. Moreover, in the same section we test one of the newly proposed models against its natural competitor (the underlying turbulence model) on a problem of computing the maximal drag and lift coefficients—a very popular benchmark problem in fluid flow modeling. Given the reference values for the drag and lift coefficients, we compared them with the results obtained by turbulent models with and without defect correction. The error in the new model's approximation of the reference values was 10 times less than the error in the approximation by the turbulence model without defect correction!

The two-step defect correction method, applied to modeling high Reynolds number flows seeks two consecutive approximation pairs (w_1, q_1), (w_2, q_2) of the quantity of interest (QoI). The QoI could be the velocity-pressure pair (u, p), the pair of spatially filtered velocity $\bar{u}$ and pressure p, or any other pair of functions $(h(u), g(p))$. If a turbulence model (TM) is chosen from the large eddy simulation (LES) family of models, we propose a new name, LES-C (large eddy simulation with correction, "Lessi"), for a model obtained via the following procedure.

ALGORITHM 1.1. *Turbulence modeling with correction.*

1. *If needed, rewrite the NSE system so that the velocity-pressure pair (u, p) is transformed into the QoI pair $(h(u), g(p))$:*
$$\widetilde{NSE}(QoI) = 0.$$
2. *Using the turbulence model (TM), find the defect step approximation of the QoI:*
$$TM(w_1, q_1) = 0.$$
3. *The correction step provides a more accurate approximation of the QoI, via*
$$TM(w_2, q_2) = TM(w_1, q_1) - \widetilde{NSE}(w_1, q_1).$$

As is the case with any other defect correction procedure, the algorithm above is naturally parallelizable. The left-hand sides of the defect and correction step equations have exactly the same structure; once the time marching discretization scheme is implemented for a continuous LES-C model, it suffices to know (w_1, q_1) at the current time level, in order to find (w_2, q_2). Thus, one can compute the solution of Algorithm 1.1 in parallel, using two cores, with the "trapezoidal" time marching: given the solution (w_1^n, q_1^n) at time level n, one computes (w_1^{n+1}, q_1^{n+1}) and (w_2^n, q_2^n) simultaneously on two cores. Both processors will be working on problems of the same complexity, which reduces the idle time.

The error in approximating the QoI pair $(h(u), g(p))$ has three components: the modeling error, the error due to temporal discretization, and the error due to the discretization in space. The most "ambitious" approach of utilizing Algorithm 1.1

would be to try to reduce all three components of the error in one correction step. In this paper, however, we focus on reducing the modeling error.

The proposed LES-C models are also a unique fit for fluid-fluid interaction problems at high Reynolds numbers, discussed in [15, 1]: few methods exist today, that allow for a stable decoupling of the fluid-fluid interaction problem with nonlinear rigid lid condition. Among these, only two have sound mathematical foundation—the geometric averaging (GA) method of [15] and the method of [39]; the GA is more computationally attractive, as it requires fewer function evaluations per time step. Thus, if one seeks a stable partitioned method, which would be higher order accurate in time, the deferred correction approach of [1] is the only alternative. If one wants to have a built-in turbulence model in the decoupling method for fluid-fluid interaction, then a LES-C model should be the most natural candidate: the extra computational cost due to the addition of the correction step is already unavoidable, as the deferred correction procedure is part of the partitioning method [1]. Moreover, as demonstrated by the numerical examples in section 4, this "extra computational cost" is deferred by the parallelizability of the defect correction procedure, and the resulting model can outperform its one-step competitors in terms of achievable accuracy per computational time.

2. Derivation of the model. When approximating the motion of an incompressible turbulent fluid flow, the modeling error plays the key role in the construction of a qualitatively and quantitatively correct solution. In order to demonstrate the effectiveness and high physical fidelity of a LES-C model, we start by choosing a LES turbulence model, which we will "correct" using Algorithm 1.1. We choose the approximate deconvolution model (ADM), introduced by Stolz and Adams [47], for the following reasons. First, the ADM models have a sound mathematical foundation, with full numerical analysis of the ADM available in the literature. They are widely used in real-life engineering applications [42]. A variety of new models appear that use the approximate deconvolution idea (in the form of the van Cittert algorithm, Tikhonov regularization, etc.) to create a blend of the ADM with other models (Leray-deconvolution model [36]) or an ADM-based reduced order model [9, 51].

Another reason for focusing on the ADM and creating the approximate deconvolution model with correction (ADC, a member of the proposed LES-C family) is the following. Most of the benchmark problems in turbulence are created to test the model's ability to approximate the velocity field u, whereas the ADM seeks to approximate $\bar{u}$—the spatially filtered velocity field. Thus, the problem of validating the ADC model becomes even more challenging, and the numerical results will be even more convincing.

2.1. Notation and preliminaries. Throughout the paper, the norm $\|\cdot\|$ denotes the usual $L^2(\Omega)$-norm of scalars, vectors, and tensors, induced by the usual L^2 inner-product, denoted by $(\cdot,\cdot)$. The space that the velocity (at time t) belongs to is given by

$$X = H_0^1(\Omega)^d = \left\{v \in L^2(\Omega)^d : \nabla v \in L^2(\Omega)^{d\times d} \text{ and } v = 0 \text{ on } \partial\Omega\right\}$$

equipped with the norm $\|v\|_X = \|\nabla v\|$. The space dual to X is equipped with the norm

$$\|f\|_{-1} = \sup_{v\in X} \frac{(f,v)}{\|\nabla v\|}.$$

The pressure (at time t) is sought in the space

$$Q = L_0^2(\Omega) = \left\{ q : q \in L^2(\Omega), \int_\Omega q(x)dx = 0 \right\}.$$

Also introduce the space of weakly divergence-free functions

$$V = \{v \in X : (\nabla \cdot v, q) = 0 \quad \forall q \in Q\}.$$

For measurable $v : [0,T] \to X$, define

$$\|v\|_{L^p(0,T;X)} = \left(\int_0^T \|v(t)\|_X^p dt \right)^{\frac{1}{p}}, \ 1 \le p < \infty,$$

and

$$\|v\|_{L^\infty(0,T;X)} = ess \sup_{0 \le t \le T} \|v(t)\|_X.$$

Define the trilinear form on $X \times X \times X$

$$b(u,v,w) = \int_\Omega u \cdot \nabla v \cdot w dx.$$

Throughout the paper, we shall assume that the velocity-pressure finite element spaces $X^h \subset X$ and $Q^h \subset Q$ are conforming and satisfy the discrete inf-sup, or LBB^h, condition. One of the most commonly used choices is the Taylor–Hood (P_2, P_1) pair of piecewise quadratic polynomials for the velocity and piecewise linears for the pressure.

The idea of approximate deconvolution modeling is based on the definition and properties of the following operator.

DEFINITION 1 (approximate deconvolution operator). *For a fixed finite N, define the Nth approximate deconvolution operator G_N by*

$$G_N \phi = \sum_{n=0}^{N} \left(I - A^{-1} \right)^n \phi,$$

where the averaging operator A^{-1} is the differential filter: given $\phi \in L^2(\Omega)$, $\overline{\phi}^\delta \in H^2(\Omega)$ is the unique solution of

$$A\overline{\phi}^\delta := -\delta^2 \Delta \overline{\phi}^\delta + \overline{\phi}^\delta = \phi \quad in\ \Omega, \tag{2.1}$$

subject to zero (or periodic) boundary conditions. Under zero (or periodic) boundary conditions, this averaging operator commutes with differentiation.

LEMMA 1. *The operator G_N is compact, is positive, and is an asymptotic inverse to the filter A^{-1}, i.e., for very smooth ϕ and as $\delta \to 0$, it satisfies*

$$\phi = G_N \overline{\phi}^\delta + (-1)^{N+1} \delta^{2N+2} \Delta^{N+1} A^{-(N+1)} \phi. \tag{2.2}$$

The proof of Lemma 1 can be found in [16].

Define the explicitly skew-symmetrized trilinear form

$$b^*(u,v,w) := \frac{1}{2}(u \cdot \nabla v, w) - \frac{1}{2}(u \cdot \nabla w, v).$$

The proofs will also require bounds on the nonlinearity.

LEMMA 2 (bounds on the nonlinear term). *Let $\Omega \subset \mathbb{R}^d$, $d = 2, 3$. There exists a constant $C = C(\Omega)$ such that $\forall\ u, v, w \in X$*

$$|b^*(u, v, w)| \leq C(\Omega)\|\nabla u\|\|\nabla v\|\|\nabla w\|. \tag{2.3}$$

Also, the following sharper bound is valid:

$$|b^*(u, v, w)| \leq C(\Omega)\sqrt{\|u\|\|\nabla u\|}\|\nabla v\|\|\nabla w\|. \tag{2.4}$$

Proof. See [21]. The sharper upper bound is improvable in $\mathbb{R}^2$. ∎

We also define the following norm, induced by the deconvolution operator A:

$$\|\phi\|_A^2 = \|\phi\|^2 + \delta^2\|\nabla\phi\|^2.$$

The following discrete Gronwall's lemma (see, e.g., [25]) will be utilized in the subsequent analysis.

LEMMA 3 (Gronwall's lemma). *Let k, M, and $a_\mu, b_\mu, c_\mu, \gamma_\mu$, for integers $\mu > 0$, be nonnegative numbers such that*

$$a_n + k\sum_{\mu=0}^{n} b_\mu \leq k\sum_{\mu=0}^{n} \gamma_\mu a_\mu + k\sum_{\mu=0}^{n} c_\mu + M \text{ for } n \geq 0. \tag{2.5}$$

Suppose that $k\gamma_\mu < 1, \forall\mu$, and set $\sigma_\mu \equiv (1 - k\gamma_\mu)^{-1}$. Then,

$$a_n + k\sum_{\mu=0}^{n} b_\mu \leq exp\left(k\sum_{\mu=0}^{n}\sigma_\mu\gamma_\mu\right)\left\{k\sum_{\mu=0}^{n} c_\mu + M\right\} \text{ for } n \geq 0. \tag{2.6}$$

The following constants and assumptions on the problem data (written here as assumptions on the true solution $\mathbf{u}$) will be used in the proofs below.

DEFINITION 2.

$$\begin{aligned} C_{\bar{u}} &:= \|\bar{u}(x,t)\|_{L^\infty(0,T;L^\infty(\Omega))}, \\ C_{\nabla\bar{u}} &:= \|\nabla\bar{u}(x,t)\|_{L^\infty(0,T;L^\infty(\Omega))}, \\ C_{\zeta} &:= \|\zeta(x,t)\|_{L^\infty(0,T;L^\infty(\Omega))}, \\ C_{\nabla\zeta} &:= \|\nabla\zeta(x,t)\|_{L^\infty(0,T;L^\infty(\Omega))}. \end{aligned}$$

2.2. Approximate deconvolution with correction. Consider the semidiscrete (continuous in time, discretized in space using the Galerkin finite element method) case. In order to create the ADC, we taylor Algorithm 1.1 to address the modeling error of the ADM.

Given the family of approximate deconvolution operators G_N and the exact deconvolution operator A from Definition 1, the solution of the Nth ADM is the pair $(w, q) \in ((X \bigcap H^2(\Omega)), Q)$ such that for any $(v, \chi) \in (X, Q)$

$$\begin{aligned} (Aw_t, v) + \nu(A\nabla w, \nabla v) + b^*(G_N w, G_N w; v) - (q, \nabla\cdot v) &= (f, v), \\ (\nabla\cdot w, \chi) &= 0. \end{aligned} \tag{2.7}$$

Consider the NSE true solution, velocity-pressure pair (u, p). The simplest ADM ($N = 0$) seeks to approximate the QoI pair $(\bar{u}, p) \in (X, Q)$ with the solution pair

$(w_1, q_1) \in (X^h, Q^h)$: find $(w_1, \zeta_1, q_1) \in (X^h, X^h, Q^h)$ such that for any $(v^h, \xi^h, \chi^h) \in (X^h, X^h, Q^h)$

$$
\begin{aligned}
(2.8) \qquad & (w_{1,t}, v^h) + \delta^2 \left(\nabla w_{1,t}, \nabla v^h\right) + \nu \left(\nabla w_1, \nabla v^h\right) + \nu\delta^2 \left(\nabla \zeta_1, \nabla v^h\right) \\
& \quad + b^* \left(w_1, w_1; v^h\right) - \left(q_1, \nabla \cdot v^h\right) = \left(f, v^h\right), \\
& \qquad\qquad \left(\nabla w_1, \nabla \xi^h\right) = \left(\zeta_1, \xi^h\right), \\
& \qquad\qquad \left(\nabla \cdot w_1, \chi^h\right) = 0,
\end{aligned}
$$

subject to $w_1(0, x) = \overline{u}_0^\delta(x)$ and no-slip boundary conditions.

Here the mixed variational formulation is implemented via the introduction of the extra variable ζ, in order to avoid the fourth order term $\nu\delta^2(\Delta w, \Delta v)$, which would lead to the usage of C^1 elements. The boundary conditions imposed for the new variable ζ_1 are $\zeta_1 = 0$ on $\partial\Omega$, because the spatial averaging operator preserves the no-slip condition.

Building the two-step ADC starts with rewriting the NSE in terms of $(\bar{u}, p)$: find $(\bar{u}, \zeta, p) \in (X^h, X^h, Q^h)$ such that for any $(v^h, \xi^h, \chi^h) \in (X^h, X^h, Q^h)$

$$
\begin{aligned}
(2.9) \qquad & \left(\bar{u}_t, v^h\right) + \delta^2 \left(\nabla \bar{u}_t, \nabla v^h\right) + \nu \left(\nabla \bar{u}, \nabla v^h\right) + \nu\delta^2 \left(\nabla \zeta, \nabla v^h\right) \\
& \quad + b^* \left(\bar{u}, \bar{u}; v^h\right) - \left(p, \nabla \cdot v^h\right) = (f, v^h) \\
& \quad - \delta^2 b^* \left(\zeta, \bar{u}; v^h\right) - \delta^2 b^* \left(\bar{u}, \zeta; v^h\right) - \delta^4 b^* \left(\zeta, \zeta; v^h\right), \\
& \qquad\qquad \left(\nabla \bar{u}, \nabla \xi^h\right) = \left(\zeta, \xi^h\right), \\
& \qquad\qquad \left(\nabla \cdot \bar{u}, \chi^h\right) = 0.
\end{aligned}
$$

Thus, the first two steps of Algorithm 1.1 are to use (2.9) as $\widetilde{NSE}(QoI) = 0$, then solve the ADM equation (2.8) in the defect step of the method. The correction step of Algorithm 1.1 now reads, Find $(w_2, \zeta_2, q_2) \in (X^h, X^h, Q^h)$ such that for any $(v^h, \xi^h, \chi^h) \in (X^h, X^h, Q^h)$

$$
\begin{aligned}
(2.10) \qquad & \left(w_{2,t}, v^h\right) + \delta^2 \left(\nabla w_{2,t}, \nabla v^h\right) + \nu \left(\nabla w_2, \nabla v^h\right) + \nu\delta^2 \left(\nabla \zeta_2, \nabla v^h\right) \\
& \quad + b^* \left(w_2, w_2; v^h\right) - \left(q_2, \nabla \cdot v^h\right) = (f, v^h) \\
& \quad - \delta^2 b^* \left(\zeta_1, w_1; v^h\right) - \delta^2 b^* \left(w_1, \zeta_1; v^h\right) - \delta^4 b^*(\zeta_1, \zeta_1; v^h), \\
& \qquad\qquad \left(\nabla w_2, \nabla \xi^h\right) = \left(\zeta_2, \xi^h\right), \\
& \qquad\qquad \left(\nabla \cdot w_2, \chi^h\right) = 0.
\end{aligned}
$$

The defect and correction steps of the ADC procedure, given by (2.8) and (2.10), respectively, have the same structure as the left-hand side. The "numerical" reasoning behind the construction of the ADC is the following: for the accuracy result of the defect step, (2.8) is subtracted from (2.9), and there is no match for the three last terms of the momentum equation of (2.9). This match is created in the correction step, thus improving the accuracy.

Even more important is to look at this from the viewpoint of conserved quantities. Compared to (2.9), the ADM formulation (2.8) seeks to "control" the flow by adding both extra energy and extra dissipation (respectively, the second and fourth terms in the left-hand side of (2.8)). Doing so, keeping the same right-hand side (power input) as in the "original" NSE flow, might lead to a flow with different qualitative behavior. The correction step aims to find a modification of the right-hand side (three extra terms that depend on the known quantities w_1, ζ_1) that should correspond to the increased energy and energy dissipation rate in the left-hand side of (2.8), (2.10).

3. Numerical analysis of the ADC. In order to investigate stability and accuracy of the ADC, we use the backward Euler's method for time discretization of (2.8)–(2.10), which leads to the following equations for $(w_1^{n+1}, \zeta_1^{n+1}, q_1^{n+1})$, $(w_2^{n+1}, \zeta_2^{n+1}, q_2^{n+1}) \in (X^h, X^h, Q^h) \forall (v^h, \xi^h, \chi^h) \in (X^h, X^h, Q^h)$ at $t = t_{n+1}$, $n \geq 0$, with $\Delta t := t_{i+1} - t_i$:

(3.1)
$$\begin{aligned}
&\left(\frac{w_1^{n+1} - w_1^n}{\Delta t}, v^h\right) + \delta^2 \left(\frac{\nabla w_1^{n+1} - \nabla w_1^n}{\Delta t}, \nabla v^h\right) + \nu \left(\nabla w_1^{n+1}, \nabla v^h\right) + \nu\delta^2 \left(\nabla \zeta_1^{n+1}, \nabla v^h\right) \\
&\quad + b^* \left(w_1^{n+1}, w_1^{n+1}; v^h\right) - \left(q_1^{n+1}, \nabla \cdot v^h\right) = \left(f(t_{n+1}), v^h\right), \\
&\qquad \left(\nabla w_1^{n+1}, \nabla \xi^h\right) = \left(\zeta_1^{n+1}, \xi^h\right), \\
&\qquad \left(\nabla \cdot w_1^{n+1}, \chi^h\right) = 0,
\end{aligned}$$

(3.2)
$$\begin{aligned}
&\left(\frac{w_2^{n+1} - w_2^n}{\Delta t}, v^h\right) + \delta^2 \left(\frac{\nabla w_2^{n+1} - \nabla w_2^n}{\Delta t}, \nabla v^h\right) + \nu \left(\nabla w_2^{n+1}, \nabla v^h\right) + \nu\delta^2 \left(\nabla \zeta_2^{n+1}, \nabla v^h\right) \\
&\quad + b^* \left(w_2^{n+1}, w_2^{n+1}; v^h\right) - \left(q_2^{n+1}, \nabla \cdot v^h\right) = \left(f\left(t_{n+1}\right), v^h\right) \\
&\quad - \delta^2 b^* \left(\zeta_1^{n+1}, w_1^{n+1}; v^h\right) - \delta^2 b^* \left(w_1^{n+1}, \zeta_1^{n+1}; v^h\right) - \delta^4 b^* \left(\zeta_1^{n+1}, \zeta_1^{n+1}; v^h\right), \\
&\qquad \left(\nabla w_2^{n+1}, \nabla \xi^h\right) = \left(\zeta_2^{n+1}, \xi^h\right), \\
&\qquad \left(\nabla \cdot w_2^{n+1}, \chi^h\right) = 0.
\end{aligned}$$

When analyzing the accuracy of the model above, the fully discrete version of (2.9) is needed:

(3.3)
$$\begin{aligned}
&\left(\frac{\bar{u}\left(t_{n+1}\right) - \bar{u}(t_n)}{\Delta t}, v^h\right) + \delta^2 \left(\frac{\nabla \bar{u}\left(t_{n+1}\right) - \nabla \bar{u}(t_n)}{\Delta t}, \nabla v^h\right) + \nu \left(\nabla \bar{u}\left(t_{n+1}\right), \nabla v^h\right) \\
&\quad + \nu\delta^2 \left(\nabla \zeta\left(t_{n+1}\right), \nabla v^h\right) + b^* \left(\bar{u}\left(t_{n+1}\right), \bar{u}\left(t_{n+1}\right); v^h\right) - \left(p(t_{n+1}), \nabla \cdot v^h\right) = \left(f(t_{n+1}), v^h\right) \\
&\quad - \delta^2 b^* \left(\zeta(t_{n+1}), \bar{u}\left(t_{n+1}\right); v^h\right) - \delta^2 b^* \left(\bar{u}\left(t_{n+1}\right), \zeta\left(t_{n+1}\right); v^h\right) - \delta^4 b^* \left(\zeta\left(t_{n+1}\right), \zeta(t_{n+1}); v^h\right) \\
&\quad + \left(\left(\frac{\bar{u}(t_{n+1}) - \bar{u}(t_n)}{\Delta t} - \bar{u}_t(t_{n+1})\right), v^h\right) + \delta^2 \left(\left(\frac{\nabla \bar{u}(t_{n+1}) - \nabla \bar{u}(t_n)}{\Delta t} - \nabla \bar{u}_t(t_{n+1})\right), \nabla v^h\right), \\
&\qquad \left(\nabla \bar{u}(t_{n+1}), \nabla \xi^h\right) = \left(\zeta(t_{n+1}), \xi^h\right), \\
&\qquad \left(\nabla \cdot \bar{u}(t_{n+1}), \chi^h\right) = 0.
\end{aligned}$$

Stability and accuracy of the ADM model (3.1) are well-established—see, e.g., the following theorems from [23].

THEOREM 1 (stability of the first approximation). *Let w_1 satisfy* (3.1). *Let $f \in L^2(0, T; H^{-1}(\Omega))$. Then, for $n = 0, \ldots, N-1$,*

$$\|w_1^{n+1}\|_A^2 + \nu \Delta t \Sigma_{i=0}^n \left\|\nabla w_1^{i+1}\right\|^2 + \nu\delta^2 \Delta t \Sigma_{i=0}^n \|\zeta_1^{i+1}\|^2 \leq \|w_1^0\|_A^2 + \frac{1}{\nu} \Delta t \Sigma_{i=0}^n \|f(t_{i+1})\|_{-1}^2.$$

THEOREM 2 (accuracy of the first approximation). *Let the time step satisfy*

$$\Delta t < \frac{\nu^3}{\max_{i=0,1,..,N} \|\nabla \bar{u}(t_i)\|^4}. \tag{3.4}$$

Let also $\bar{u} \in L^2(0,T;H^3(\Omega))$ *and* $\bar{u}_{tt} \in L^2(0,T;H^1(\Omega))$. *The error in the first approximation satisfies*

(3.5)
$$\left\|\bar{u}(t_{n+1}) - w_1^{n+1}\right\|_A^2 + \nu\Delta t \sum_{i=0}^{n} \left\|\nabla\left(\bar{u}\left(t_{i+1}\right) - w_1^{i+1}\right)\right\|^2 + \nu\delta^2\Delta t \sum_{i=0}^{n} \left\|\zeta(t_{i+1}) - \zeta_1^{i+1}\right\|^2$$
$$\leq C\left(\Delta t^2 + \delta^4 + \Delta t \sum_{i=0}^{n}\left(\left(1+\delta^2 h^{-2}\right)\inf_{v\in V^h}\left\|\nabla\left(\bar{u}(t_i) - v^i\right)\right\|^2 + \inf_{q\in Q^h}\|p(t_i) - q^i\|^2\right)\right).$$

It is common to see Taylor–Hood finite elements employed in real-life applications that involve turbulent flows. It is also common practice to take the filtering width to be equal to the least resolvable spatial scale, the mesh diameter: $\delta = h$. In this case, the ADM model (3.1) is first order accurate in time and second order accurate with respect to the mesh diameter and the filtering width. With the three extra terms in the right-hand side of the correction step momentum equation of (3.2), and with increased regularity assumptions on the true solution, we aim to improve the accuracy with respect to the filtering width.

The following result is needed for investigation of the accuracy of the correction step approximation.

THEOREM 3 (accuracy of the Laplacian). *Let the assumptions of Theorem* 2 *be satisfied. Let also* $\bar{u} \in L^\infty(0,T;L^\infty(\Omega))$, $\nabla\bar{u} \in L^\infty(0,T;L^\infty(\Omega))$, $\Delta\bar{u} \in L^2(0,T;H^1(\Omega))\cap L^\infty(0,T;L^\infty(\Omega))$, $\nabla\bar{u}_{tt} \in L^2(0,T;H^1(\Omega))$. *Let the time step and the filtering width satisfy* $\Delta t \leq h^{1/2}, \delta \leq h^{1/4}$. *Then the following accuracy result holds for the solution* $(w_1^{n+1}, \zeta_1^{n+1}, q_1^{n+1})$ *of* (3.1)*:*

(3.6)
$$\left\|\nabla\left(\bar{u}\left(t_{n+1}\right) - w_1^{n+1}\right)\right\|^2 + \delta^2\left\|\zeta(t_{n+1}) - \zeta_1^{n+1}\right\|^2 + \nu\Delta t\sum_{i=0}^{n}\left\|\zeta(t_{i+1}) - \zeta_1^{i+1}\right\|^2$$
$$+ \nu\delta^2\Delta t\sum_{i=0}^{n}\left\|\nabla\left(\zeta(t_{i+1}) - \zeta_1^{i+1}\right)\right\|^2 \leq C\left(\Delta t^2 + \Delta t^2\delta^2 + \delta^4 + \Delta t\sum_{i=0}^{n}\right.$$
$$\left.\times\left(\inf_{v\in V^h}\left\|\nabla\left(\bar{u}(t_i) - v^i\right)\right\|^2 + \inf_{r\in V^h}\|\zeta(t_i) - r^i\|^2 + \min(\delta^{-2}, h^{-2})\cdot\inf_{q\in Q^h}\|p(t_i) - q^i\|^2\right)\right).$$

Proof. Start with the backward Euler method for NSE, (3.3); subtract (3.1) and choose $v^h = \psi^{n+1}$, where $\zeta(t_{n+1}) - \zeta_1^{n+1} = \psi^{n+1} - \mu^{n+1}$, $\psi^{n+1} \in V^h$. Using also the error decomposition $e_1^{n+1} = \bar{u}(t_{n+1}) - w_1^{n+1} = \phi^{n+1} - \eta^{n+1}$, $\phi^{n+1} \in V^h$, we obtain

(3.7)
$$\left(\frac{\phi^{n+1} - \phi^n}{\Delta t}, \psi^{n+1}\right) - \left(\frac{\eta^{n+1} - \eta^n}{\Delta t}, \psi^{n+1}\right)$$
$$+ \delta^2\left(\frac{\nabla\phi^{n+1} - \nabla\phi^n}{\Delta t}, \nabla\psi^{n+1}\right) - \delta^2\left(\frac{\nabla\eta^{n+1} - \nabla\eta^n}{\Delta t}, \nabla\psi^{n+1}\right)$$
$$+ \nu\left(\nabla\phi^{n+1}, \nabla\psi^{n+1}\right) - \nu\left(\nabla\eta^{n+1}, \nabla\psi^{n+1}\right) + \nu\delta^2\|\nabla\psi^{n+1}\|^2 - \nu\delta^2\left(\nabla\mu^{n+1}, \nabla\psi^{n+1}\right)$$
$$+ b^*\left(\bar{u}(t_{n+1}) - w_1^{n+1}, \bar{u}(t_{n+1}); \psi^{n+1}\right) - b^*\left(w_1^{n+1}, \bar{u}(t_{n+1}) - w_1^{n+1}; \psi^{n+1}\right)$$
$$- \left(q(t_{n+1}) - q_1^{n+1}, \nabla\cdot\psi^{n+1}\right) = -\delta^2 b^*\left(\zeta(t_{n+1}), \bar{u}(t_{n+1}); \psi^{n+1}\right)$$
$$- \delta^2 b^*\left(\bar{u}(t_{n+1}), \zeta(t_{n+1}); \psi^{n+1}\right) - \delta^4 b^*\left(\zeta(t_{n+1}), \zeta(t_{n+1}); \psi^{n+1}\right)$$

$$+\left(\left(\frac{\bar{u}(t_{n+1})-\bar{u}(t_n)}{\Delta t}-\bar{u}_t(t_{n+1})\right),\psi^{n+1}\right)$$
$$+\delta^2\left(\left(\frac{\nabla\bar{u}(t_{n+1})-\nabla\bar{u}(t_n)}{\Delta t}-\nabla\bar{u}_t(t_{n+1})\right),\nabla\psi^{n+1}\right).$$

The following equalities can be derived with appropriate choices of ξ^h in the definitions of ζ and ζ_1:

$$(\psi^i,\phi^j)=(\mu^i,\phi^j)+(\nabla\phi^i,\nabla\phi^j)-(\nabla\eta^i,\nabla\phi^j)\qquad\forall i,j, \tag{3.8}$$
$$(\nabla\phi^i,\nabla\psi^j)=(\nabla\eta^i,\nabla\psi^j)+(\psi^i,\psi^j)-(\mu^i,\psi^j).$$

Using (3.7)–(3.8) leads to

$$\begin{aligned}&\frac{\|\nabla\phi^{n+1}\|^2-\|\nabla\phi^n\|^2}{2\Delta t}+\delta^2\frac{\|\psi^{n+1}\|^2-\|\psi^n\|^2}{2\Delta t}+\nu\|\psi^{n+1}\|^2+\nu\delta^2\|\nabla\psi^{n+1}\|^2\\&\quad\le-\left(\mu^{n+1},\frac{\phi^{n+1}-\phi^n}{\Delta t}\right)+\left(\nabla\eta^{n+1},\nabla\left(\frac{\phi^{n+1}-\phi^n}{\Delta t}\right)\right)+\left(\frac{\eta^{n+1}-\eta^n}{\Delta t},\psi^{n+1}\right)\\&\qquad-\delta^2\left(\frac{\mu^{n+1}-\mu^n}{\Delta t},\psi^{n+1}\right)+\nu\left(\mu^{n+1},\psi^{n+1}\right)+\nu\delta^2\left(\nabla\mu^{n+1},\nabla\psi^{n+1}\right)\\&\qquad+\left(\left(\frac{\bar{u}(t_{n+1})-\bar{u}(t_n)}{\Delta t}-\bar{u}_t(t_{n+1})\right),\psi^{n+1}\right)\\&\qquad+\delta^2\left(\left(\frac{\nabla\bar{u}(t_{n+1})-\nabla\bar{u}(t_n)}{\Delta t}-\nabla\bar{u}_t(t_{n+1})\right),\nabla\psi^{n+1}\right)\\&\qquad+\left(q(t_{n+1})-q_1^{n+1},\nabla\cdot\psi^{n+1}\right)-b^*\left(\bar{u}(t_{n+1})-w_1^{n+1},\bar{u}(t_{n+1});\psi^{n+1}\right)\\&\qquad+b^*\left(w_1^{n+1},\bar{u}(t_{n+1})-w_1^{n+1};\psi^{n+1}\right)-\delta^2b^*\left(\zeta(t_{n+1}),\bar{u}(t_{n+1});\psi^{n+1}\right)\\&\qquad-\delta^2b^*\left(\bar{u}(t_{n+1}),\zeta(t_{n+1});\psi^{n+1}\right)-\delta^4b^*\left(\zeta(t_{n+1}),\zeta(t_{n+1});\psi^{n+1}\right).\end{aligned} \tag{3.9}$$

The Cauchy–Schwarz inequality, along with the error bound for the time derivative $\frac{e_1^{n+1}-e_1^n}{\Delta t}$ from Theorem 3.3 of [23], is used to treat the first eight terms in the right-hand side of (3.9):

$$\begin{aligned}&\frac{\|\nabla\phi^{n+1}\|^2-\|\nabla\phi^n\|^2}{2\Delta t}+\delta^2\frac{\|\psi^{n+1}\|^2-\|\psi^n\|^2}{2\Delta t}+\nu\|\psi^{n+1}\|^2+\nu\delta^2\|\nabla\psi^{n+1}\|^2\\&\quad\le\frac{1}{2}\left\|\frac{\phi^{n+1}-\phi^n}{\Delta t}\right\|^2+\frac{1}{2}\|\mu^{n+1}\|^2+\nu\left\|\frac{\phi^{n+1}-\phi^n}{\Delta t}\right\|^2\\&\qquad+\frac{C}{\nu}\|\nabla\eta^{n+1}\|^2+3\epsilon\nu\|\psi^{n+1}\|^2+\frac{C}{\nu}\left\|\frac{\eta^{n+1}-\eta^n}{\Delta t}\right\|^2\\&\qquad+\frac{C}{\nu}\delta^4\left\|\frac{\mu^{n+1}-\mu^n}{\Delta t}\right\|^2+C\nu\|\mu^{n+1}\|^2+\epsilon_1\nu\delta^2\|\nabla\psi^{n+1}\|^2+C\nu\delta^2\|\nabla\mu^{n+1}\|^2\\&\qquad+\epsilon\nu\|\psi^{n+1}\|^2+\frac{C}{\nu}\Delta t^2\|\bar{u}_{tt}(t_{n+\theta})\|^2+\epsilon_1\nu\delta^2\|\nabla\psi^{n+1}\|^2+\frac{C}{\nu}\delta^2\Delta t^2\|\nabla\bar{u}_{tt}(t_{n+\theta})\|^2\\&\qquad+\left(q(t_{n+1})-q_1^{n+1},\nabla\cdot\psi^{n+1}\right)-b^*\left(\bar{u}(t_{n+1})-w_1^{n+1},\bar{u}(t_{n+1});\psi^{n+1}\right)\\&\qquad+b^*\left(w_1^{n+1},\bar{u}(t_{n+1})-w_1^{n+1};\psi^{n+1}\right)-\delta^2b^*\left(\zeta(t_{n+1}),\bar{u}(t_{n+1});\psi^{n+1}\right)\\&\qquad-\delta^2b^*\left(\bar{u}(t_{n+1}),\zeta(t_{n+1});\psi^{n+1}\right)-\delta^4b^*\left(\zeta(t_{n+1}),\zeta\left(t_{n+1}\right);\psi^{n+1}\right).\end{aligned} \tag{3.10}$$

The pressure term is bounded, based on the comparison of δ and h: if $\delta \leq h$,

$$\left(q(t_{n+1}) - q_1^{n+1}, \nabla \cdot \psi^{n+1}\right) \leq \epsilon\nu \|\psi^{n+1}\|^2 + \frac{Ch^{-2}}{\nu}\|q(t_{n+1}) - q_1^{n+1}\|^2. \tag{3.11}$$

Otherwise, if $\delta \geq h$, use

$$\left(q(t_{n+1}) - q_1^{n+1}, \nabla \cdot \psi^{n+1}\right) \leq \epsilon_1\nu\delta^2 \|\nabla\psi^{n+1}\|^2 + \frac{C\delta^{-2}}{\nu}\left\|q(t_{n+1}) - q_1^{n+1}\right\|^2. \tag{3.12}$$

Finally, the five nonlinear terms from the right-hand side of (3.10) are bounded below, using Young's inequality; terms in parentheses are bounded by Theorem 2 (either immediately or after summation over the time levels and multiplication by Δt).

$$\begin{aligned}\left|b^*\left(\bar{u}(t_{n+1}) - w_1^{n+1}, \bar{u}(t_{n+1}); \psi^{n+1}\right)\right| \\ \leq \epsilon\nu\|\psi^{n+1}\|^2 + \frac{C \cdot C_{\nabla\bar{u}}}{\nu^2}\left(\nu\left\|\nabla(\bar{u}(t_{n+1}) - w_1^{n+1})\right\|^2\right),\end{aligned} \tag{3.13}$$

$$\begin{aligned}&\left|b^*\left(w_1^{n+1}, \bar{u}(t_{n+1}) - w_1^{n+1}; \psi^{n+1}\right)\right| \\ &\quad\leq \left|b^*\left(\bar{u}(t_{n+1}), \bar{u}(t_{n+1}) - w_1^{n+1}; \psi^{n+1}\right)\right| + \left|b^*\left(\bar{u}(t_{n+1}) - w_1^{n+1}, \bar{u}(t_{n+1}) - w_1^{n+1}; \psi^{n+1}\right)\right| \\ &\quad\leq \epsilon\nu\|\psi^{n+1}\|^2 + \frac{C \cdot C_{\bar{u}}}{\nu^2}\left(\nu\left\|\nabla(\bar{u}(t_{n+1}) - w_1^{n+1})\right\|^2\right) \\ &\qquad + \epsilon\nu\|\psi^{n+1}\|^2 + \frac{C}{\nu}\|\bar{u}(t_{n+1}) - w_1^{n+1}\|\left\|\nabla\left(\bar{u}(t_{n+1}) - w_1^{n+1}\right)\right\|^3 \\ &\quad\leq 2\epsilon\nu\|\psi^{n+1}\|^2 + \frac{C \cdot C_{\bar{u}}}{\nu^2}\left(\nu\|\nabla\left(\bar{u}(t_{n+1}) - w_1^{n+1}\right)\|^2\right) \\ &\qquad + \frac{C}{\nu^2}\left(\|\bar{u}(t_{n+1}) - w_1^{n+1}\|^2 h^{-1}\right)\left(\nu\|\nabla\left(\bar{u}(t_{n+1}) - w_1^{n+1}\right)\|^2\right).\end{aligned} \tag{3.14}$$

In the last step of (3.14) an inverse inequality was used in the following manner:

$$\begin{aligned}&\left\|\nabla\left(\bar{u}(t_{n+1}) - w_1^{n+1}\right)\right\| \leq \|\nabla\left(\bar{u}\left(t_{n+1}\right) - \bar{U_h}\right)\| + \|\nabla(\bar{U_h} - w_1^{n+1})\| = \|\nabla\bar{\eta}\| + \|\nabla\bar{\phi}\| \\ &\quad\leq \|\nabla\bar{\eta}\| + h^{-1}\|\bar{\phi}\|, \text{ for } \bar{U_h} \in X^h.\end{aligned} \tag{3.15}$$

The expression in the first parentheses in the last line of (3.14) is bounded uniformly in time via Theorem 2. The expression in the last parentheses is also bounded by the same theorem, after summation over the time levels and multiplication by Δt.

We now proceed with the treatment of the remaining trilinear terms.

$$|\delta^2 b^*(\zeta(t_{n+1}), \bar{u}(t_{n+1}); \psi^{n+1})| \leq \epsilon\nu\|\psi^{n+1}\|^2 + \frac{C \cdot C_{\nabla\bar{u}}}{\nu}\|\nabla\zeta(t_{n+1})\|^2\delta^4. \tag{3.16}$$

$$|\delta^2 b^*(\bar{u}(t_{n+1}), \zeta(t_{n+1}); \psi^{n+1})| \leq \epsilon\nu\|\psi^{n+1}\|^2 + \frac{C \cdot C_{\bar{u}}}{\nu}\|\nabla\zeta(t_{n+1})\|^2\delta^4. \tag{3.17}$$

$$|\delta^4 b^*(\zeta(t_{n+1}), \zeta(t_{n+1}); \psi^{n+1})| \leq \epsilon\nu\|\psi^{n+1}\|^2 + \frac{C_\zeta}{\nu}\|\nabla\zeta(t_{n+1})\|^2\delta^4. \tag{3.18}$$

Take $\epsilon = \frac{1}{22}, \epsilon_1 = \frac{1}{6}$. Multiplying by $2\Delta t$, summing over the time levels, and using the triangle inequality completes the proof. ∎

We now proceed to proving stability and accuracy of the correction step approximation.

THEOREM 4 (stability of the ADC). *Let w_2 satisfy* (3.2). *Let the assumptions of Theorem* 3 *be satisfied; let also $\Delta\bar{u} \in L^\infty(0,T;H^1(\Omega))$. Then there exists C independent of $h, \Delta t$ such that, for $n = 0, \dots, N-1$,*

$$\|w_2^{n+1}\|_A^2 + \nu\Delta t\Sigma_{i=0}^n\|\nabla w_2^{i+1}\|^2 + \nu\delta^2\Delta t\Sigma_{i=0}^n\|\zeta_2^{i+1}\|^2 \le \frac{C}{\nu^2}\left(\|w_2^0\|_A^2 + \frac{1}{\nu}\Delta t\Sigma_{i=0}^n\|f(t_{i+1})\|_{-1}^2\right).$$

Proof. Take $v^h = w_2^{n+1}$ in (3.2) and use the Cauchy-Schwarz inequality, bounds from Lemma 2, and Young's inequality to obtain

$$\begin{aligned}(3.19)\quad &\frac{\|w_2^{n+1}\|^2 - \|w_2^n\|^2}{2\Delta t} + \delta^2\frac{\|\nabla w_2^{n+1}\|^2 - \|\nabla w_2^n\|^2}{2\Delta t} + \nu\|\nabla w_2^{n+1}\|^2 + \nu\delta^2\|\zeta_2^{n+1}\|^2 \\ &\le \epsilon\nu\|\nabla w_2^{n+1}\|^2 + \frac{1}{4\epsilon\nu}\|f(t_{n+1})\|_{-1}^2 \\ &\quad + 2\epsilon\nu\|\nabla w_2^{n+1}\|^2 + \frac{C}{\nu^2}\left(\delta^2\|\nabla w_1^{n+1}\|^2\right)\left(\nu\delta^2\|\nabla\zeta_1^{n+1}\|^2\right) \\ &\quad + \epsilon\nu\|\nabla w_2^{n+1}\|^2 + \frac{C}{\nu^2}\delta^6\|\nabla\zeta(t_{n+1})\|^2\left(\nu\delta^2\|\nabla\zeta_1^{n+1}\|^2\right) \\ &\quad + \epsilon\nu\|\nabla w_2^{n+1}\|^2 + \frac{C}{\nu^2}\frac{\delta^4}{h}\left(\delta^2\|\zeta(t_{n+1}) - \zeta_1^{n+1}\|^2\right)\left(\nu\delta^2\|\nabla\zeta_1^{n+1}\|^2\right).\end{aligned}$$

Taking $\epsilon = \frac{1}{10}$, multiplying (3.19) by $2\Delta t$, summing over the time levels, and utilizing the results of Theorems 1 and 3 completes the proof. ∎

THEOREM 5 (accuracy of the ADC). *Let the assumptions of Theorem* 3 *be satisfied. Let also $\nabla(\Delta\bar{u}) \in L^\infty(0,T;L^\infty(\Omega))$. Then the accuracy of the correction step approximation is given by*

$$\begin{aligned}(3.20)\quad &\|\bar{u}(t_{n+1}) - w_2^{n+1}\|_A^2 + \nu\Delta t\sum_{i=0}^n\left\|\nabla\left(\bar{u}(t_{i+1}) - w_2^{i+1}\right)\right\|^2 \\ &+ \nu\delta^2\Delta t\sum_{i=0}^n\|\zeta(t_{i+1}) - \zeta_2^{i+1}\|^2 \le C\Bigg(\Delta t^2 + \Delta t^2\delta^4 + \delta^8 + \Delta t\sum_{i=0}^n\Bigg(\left(1 + \nu\delta^2h^{-2}\right) \\ &\inf_{v^h\in V^h}\left\|\nabla\left(\bar{u}(t_i) - v^h\right)\right\|^2 + \inf_{r^h\in V^h}\left\|\zeta(t_i) - r^h\right\|^2 + \inf_{q^h\in Q^h}\left\|p(t_i) - q^h\right\|^2\Bigg)\Bigg).\end{aligned}$$

Proof. Let $e_2^i = \bar{u}(t_i) - w_2^i = \phi^i - \eta^i$, where $\phi \in V^h$. Let also $\zeta(t_i) - \zeta_2^i = \psi^i - \mu^i$, with $\psi \in V^h$.

Subtract (3.2) from (3.3), and take $v^h = \phi^{n+1}$ to obtain

$$\begin{aligned}(3.21)\quad &\left(\frac{\phi^{n+1} - \phi^n}{\Delta t}, \phi^{n+1}\right) - \left(\frac{\eta^{n+1} - \eta^n}{\Delta t}, \phi^{n+1}\right) \\ &+ \delta^2\left(\frac{\nabla\phi^{n+1} - \nabla\phi^n}{\Delta t}, \nabla\phi^{n+1}\right) - \delta^2\left(\frac{\nabla\eta^{n+1} - \nabla\eta^n}{\Delta t}, \nabla\phi^{n+1}\right) \\ &+ \nu\|\nabla\phi^{n+1}\|^2 - \nu\left(\nabla\eta^{n+1}, \nabla\phi^{n+1}\right) + \nu\delta^2\left(\nabla\psi^{n+1}, \nabla\phi^{n+1}\right) \\ &- \nu\delta^2\left(\nabla\mu^{n+1}, \nabla\phi^{n+1}\right) - \left(q(t_{n+1}) - q_2^{n+1}, \nabla\cdot\phi^{n+1}\right)\end{aligned}$$

$$
\begin{aligned}
&+ b^*\left(\bar{u}(t_{n+1}) - w_2^{n+1}, \bar{u}(t_{n+1}); \phi^{n+1}\right) + b^*\left(w_2^{n+1}, \bar{u}(t_{n+1}) - w_2^{n+1}; \phi^{n+1}\right)\\
&= -\delta^2\left(b^*\left(\zeta(t_{n+1}), \bar{u}(t_{n+1}); \phi^{n+1}\right) - b^*\left(\zeta_1^{n+1}, w_1^{n+1}; \phi^{n+1}\right)\right)\\
&\quad - \delta^2\left(b^*\left(\bar{u}(t_{n+1}), \zeta(t_{n+1}); \phi^{n+1}\right) - b^*\left(w_1^{n+1}, \zeta_1^{n+1}; \phi^{n+1}\right)\right)\\
&\quad - \delta^4\left(b^*\left(\zeta(t_{n+1}), \zeta(t_{n+1}); \phi^{n+1}\right) - b^*\left(\zeta_1^{n+1}, \zeta_1^{n+1}; \phi^{n+1}\right)\right)\\
&\quad + \left(\left(\frac{\bar{u}(t_{n+1}) - \bar{u}(t_n)}{\Delta t} - \bar{u}_t(t_{n+1})\right), \phi^{n+1}\right)\\
&\quad + \delta^2\left(\left(\frac{\nabla\bar{u}(t_{n+1}) - \nabla\bar{u}(t_n)}{\Delta t} - \nabla\bar{u}_t(t_{n+1})\right), \nabla\phi^{n+1}\right).
\end{aligned}
$$

Applying the Cauchy–Schwarz inequality gives

$$
\begin{aligned}
&\frac{\|\phi^{n+1}\|^2 - \|\phi^n\|^2}{2\Delta t} + \delta^2\frac{\|\nabla\phi^{n+1}\|^2 - \|\nabla\phi^n\|^2}{2\Delta t}\\
&\quad + \nu\|\nabla\phi^{n+1}\|^2 + \nu\delta^2\|\psi^{n+1}\|^2\\
&\le 5\nu\epsilon\|\nabla\phi^{n+1}\|^2 + \frac{1}{4\epsilon\nu}\left\|\frac{\eta^{n+1} - \eta^n}{\Delta t}\right\|_{-1}^2 + \frac{1}{4\epsilon\nu}\delta^4\left\|\frac{\nabla\eta^{n+1} - \nabla\eta^n}{\Delta t}\right\|^2\\
&\quad + \frac{1}{4\epsilon}\|\nabla\eta^{n+1}\|^2 + \frac{1}{4\epsilon}\nu\delta^4\|\nabla\mu^{n+1}\|^2 + \frac{1}{4\epsilon}\inf_{q^h\in Q^h}\|p(t_{n+1}) - q^h\|^2\\
&\quad + 2\nu\delta^2\epsilon_1\|\psi^{n+1}\|^2 + \frac{1}{4\epsilon_1}\nu\delta^2\|\Delta\eta^{n+1}\|^2 + \frac{1}{4\epsilon_1}\nu\delta^2\|\mu^{n+1}\|^2\\
&\quad + 2\epsilon\nu\|\phi^{n+1}\|^2 + \frac{C}{\nu}\Delta t^2\|\bar{u}_{tt}(t_{n+\theta})\|^2 + \frac{C}{\nu}\delta^4\Delta t^2\|\nabla\bar{u}_{tt}(t_{n+\theta})\|^2\\
&\quad + \left|b^*\left(\bar{u}(t_{n+1}) - w_2^{n+1}, \bar{u}(t_{n+1}); \phi^{n+1}\right) + b^*\left(w_2^{n+1}, \bar{u}(t_{n+1}) - w_2^{n+1}; \phi^{n+1}\right)\right|\\
&\quad + \delta^2\left|b^*\left(\zeta(t_{n+1}), \bar{u}(t_{n+1}); \phi^{n+1}\right) - b^*\left(\zeta_1^{n+1}, w_1^{n+1}; \phi^{n+1}\right)\right|\\
&\quad + \delta^2\left|b^*\left(\bar{u}\left(t_{n+1}\right), \zeta(t_{n+1}); \phi^{n+1}\right) - b^*\left(w_1^{n+1}, \zeta_1^{n+1}; \phi^{n+1}\right)\right|\\
&\quad + \delta^4\left|b^*\left(\zeta(t_{n+1}), \zeta(t_{n+1}); \phi^{n+1}\right) - b^*\left(\zeta_1^{n+1}, \zeta_1^{n+1}; \phi^{n+1}\right)\right|.
\end{aligned} \tag{3.22}
$$

Next, the four pairs of trilinear terms will be bounded, using Lemma 2, Young's inequality, regularity assumptions on the true solution, and the results of Theorem 3.

$$
\begin{aligned}
&\left|b^*\left(\bar{u}(t_{n+1}) - w_2^{n+1}, \bar{u}(t_{n+1}); \phi^{n+1}\right) + b^*\left(w_2^{n+1}, \bar{u}(t_{n+1}) - w_2^{n+1}; \psi^{n+1}\right)\right|\\
&\quad = \left|b^*\left(\phi^{n+1}, \bar{u}(t_{n+1}); \phi^{n+1}\right) - b^*\left(\eta^{n+1}, \bar{u}(t_{n+1}); \phi^{n+1}\right) - b^*\left(w_2^{n+1}, \eta^{n+1}; \phi^{n+1}\right)\right|\\
&\quad = \left|b^*\left(\phi^{n+1}, \bar{u}(t_{n+1}); \phi^{n+1}\right) - b^*\left(\eta^{n+1}, \bar{u}(t_{n+1}); \phi^{n+1}\right)\right.\\
&\qquad \left. - b^*\left(\bar{u}(t_{n+1}), \eta^{n+1}; \phi^{n+1}\right) + b^*\left(\phi^{n+1}, \eta^{n+1}; \phi^{n+1}\right) - b^*\left(\eta^{n+1}, \eta^{n+1}; \phi^{n+1}\right)\right|.
\end{aligned} \tag{3.23}
$$

The bounds on each of the five terms in (3.23) are as follows:

$$
\begin{aligned}
\left|b^*\left(\phi^{n+1}, \bar{u}(t_{n+1}); \phi^{n+1}\right)\right| &\le \epsilon\nu\|\nabla\phi^{n+1}\|^2 + \frac{C\cdot C_{\nabla\bar{u}}}{\nu}\|\phi^{n+1}\|^2,\\
\left|b^*\left(\eta^{n+1}, \bar{u}(t_{n+1}); \phi^{n+1}\right)\right| &\le \epsilon\nu\|\nabla\phi^{n+1}\|^2 + \frac{C}{\nu}\|\nabla\bar{u}(t_{n+1})\|^2\|\nabla\eta^{n+1}\|^2,\\
\left|b^*\left(\bar{u}(t_{n+1}), \eta^{n+1}; \phi^{n+1}\right)\right| &\le \epsilon\nu\|\nabla\phi^{n+1}\|^2 + \frac{C}{\nu}\|\nabla\bar{u}(t_{n+1})\|^2\|\nabla\eta^{n+1}\|^2,\\
\left|b^*\left(\phi^{n+1}, \eta^{n+1}; \phi^{n+1}\right)\right| &\le C\|\phi^{n+1}\|^{\frac{1}{2}}\|\nabla\eta^{n+1}\|\|\nabla\phi^{n+1}\|^{\frac{3}{2}}\\
&\le \epsilon\nu\|\nabla\phi^{n+1}\|^2 + C\nu^{-3}\|\nabla\eta^{n+1}\|^4\|\phi^{n+1}\|^2,\\
\left|b^*\left(\eta^{n+1}, \eta^{n+1}; \phi^{n+1}\right)\right| &\le \epsilon\nu\|\nabla\phi^{n+1}\|^2 + \frac{C}{\nu}\|\nabla\eta^{n+1}\|^4.
\end{aligned} \tag{3.24}
$$

Finally, these are the bounds on the remaining three pairs of trilinear terms in (3.22):

(3.25)

$$\begin{aligned}
&\delta^2\left|b^*\left(\zeta(t_{n+1}),\bar{u}(t_{n+1});\phi^{n+1}\right)-b^*\left(\zeta_1^{n+1},w_1^{n+1};\phi^{n+1}\right)\right|\\
&\quad\le\delta^2\left|b^*\left(\zeta(t_{n+1}),\bar{u}(t_{n+1});\phi^{n+1}\right)-b^*\left(\zeta_1^{n+1},\bar{u}(t_{n+1});\phi^{n+1}\right)\right|\\
&\qquad+\delta^2\left|b^*\left(\zeta_1^{n+1},\bar{u}(t_{n+1});\phi^{n+1}\right)-b^*\left(\zeta_1^{n+1},w_1^{n+1};\phi^{n+1}\right)\right|\\
&\quad\le\epsilon\nu\|\nabla\phi^{n+1}\|^2+\frac{C\cdot C_{\nabla\bar{u}}}{\nu^2}\delta^4\left(\nu\|\zeta(t_{n+1})-\zeta_1^{n+1}\|^2\right)\\
&\qquad+\epsilon\nu\|\nabla\phi^{n+1}\|^2+\frac{C_\zeta}{\nu}\delta^4\left(\|\bar{u}(t_{n+1})-w_1^{n+1}\|^2\right)\\
&\qquad+\epsilon\nu\|\nabla\phi^{n+1}\|^2+\frac{C}{\nu^2}\delta^2\left(\nu\delta^2\|\nabla\left(\zeta(t_{n+1})-\zeta_1^{n+1}\right)\|^2\right)\left(\|\nabla\left(\bar{u}(t_{n+1})-w_1^{n+1}\right)\|^2\right),
\end{aligned}$$

(3.26)

$$\begin{aligned}
&\delta^2\left|b^*\left(\bar{u}(t_{n+1}),\zeta(t_{n+1});\phi^{n+1}\right)-b^*\left(w_1^{n+1},\zeta_1^{n+1};\phi^{n+1}\right)\right|\\
&\quad\le\delta^2\left|b^*\left(\bar{u}(t_{n+1}),\zeta(t_{n+1});\phi^{n+1}\right)-b^*\left(\bar{u}(t_{n+1}),\zeta_1^{n+1};\phi^{n+1}\right)\right|\\
&\qquad+\delta^2\left|b^*\left(\zeta_1^{n+1},\bar{u}(t_{n+1});\phi^{n+1}\right)-b^*\left(\zeta_1^{n+1},w_1^{n+1};\phi^{n+1}\right)\right|\\
&\quad\le\epsilon\nu\|\nabla\phi^{n+1}\|^2+\frac{C_{\bar{u}}}{\nu^2}\delta^4\left(\nu\|\zeta(t_{n+1})-\zeta_1^{n+1}\|^2\right)\\
&\qquad+2\epsilon\nu\|\nabla\phi^{n+1}\|^2+\frac{C_{\nabla\zeta}}{\nu}\delta^4\left(\|\bar{u}(t_{n+1})-w_1^{n+1}\|^2\right)\\
&\qquad+\frac{C}{\nu^2}\delta^2\left(\nu\delta^2\|\nabla\left(\zeta(t_{n+1})-\zeta_1^{n+1}\right)\|^2\right)\left(\|\nabla\left(\bar{u}(t_{n+1})-w_1^{n+1}\right)\|^2\right),
\end{aligned}$$

(3.27)

$$\begin{aligned}
&\delta^4\left|b^*\left(\zeta(t_{n+1}),\zeta(t_{n+1});\phi^{n+1}\right)-b^*\left(\zeta_1^{n+1},\zeta_1^{n+1};\phi^{n+1}\right)\right|\\
&\quad\le\delta^4\left|b^*\left(\zeta(t_{n+1}),\zeta(t_{n+1});\phi^{n+1}\right)-b^*\left(\zeta_1^{n+1},\zeta(t_{n+1});\phi^{n+1}\right)\right|\\
&\qquad+\delta^4\left|b^*\left(\zeta_1^{n+1},\zeta(t_{n+1});\phi^{n+1}\right)-b^*(\zeta_1^{n+1},\zeta_1^{n+1};\phi^{n+1})\right|\\
&\quad\le2\epsilon\nu\|\nabla\phi^{n+1}\|^2+\frac{C_\zeta}{\nu}\delta^6\left(\delta^2\|\zeta(t_{n+1})-\zeta_1^{n+1}\|^2\right)\\
&\qquad+\frac{C}{\nu}\delta^8\|\zeta(t_{n+1})-\zeta_1^{n+1}\|\|\nabla(\zeta(t_{n+1})-\zeta_1^{n+1})\|^3\\
&\quad\le2\epsilon\nu\|\nabla\phi^{n+1}\|^2+\frac{C_\zeta}{\nu}\delta^6\left(\delta^2\|\zeta(t_{n+1})-\zeta_1^{n+1}\|^2\right)\\
&\qquad+\frac{C\delta^4h^{-1}}{\nu^2}\left(\delta^2\|\zeta(t_{n+1})-\zeta_1^{n+1}\|^2\right)\left(\nu\delta^2\|\nabla(\zeta(t_{n+1})-\zeta_1^{n+1})\|^2\right).
\end{aligned}$$

Take $\epsilon=\frac{1}{40},\epsilon_1=\frac{1}{4}$. Multiply by $2\Delta t$, sum over the time levels, and use the discrete Gronwall's lemma, Lemma 3. Using the triangle inequality completes the proof. ∎

Thus, compared to the ADM, the modeling error of the ADC is improved from $O(\delta^2)$ to $O(\delta^4)$. Of course, in practice one would have to improve all components of the overall error, in order to fully enjoy the improved accuracy. Therefore, the real "justification" of the model's high physical fidelity can only come from the computational testing—see the next section.

4. Model validation. Before we test the ADC numerically, let's look more closely at the difference between the underlying ADM model and the ADC. In particular, we propose to apply the ADC (including the ADM as the first step) to the

Taylor–Green vortex problem. This is a well-known benchmark problem for the NSE, described, e.g., in [50, 46, 8, 34]: the flow in a 2π-periodic box with zero forcing.

The analytic solutions, called Taylor solutions (eddy solutions, general Green–Taylor solutions), can be viewed as an example of generalized Beltrami flows: see [8] for the detailed explanation, as well as the relationship between these eddy solutions and the ABC (Arnold–Beltrami–Childress) flow. This benchmark problem is of special interest to us, because of the result in [34]. There, it was shown that the Taylor solutions of the NSE are also exact solutions of the ADM. We start the validation of the ADC by checking that the new model can also capture the vortex structures of the Taylor solution.

Following the setup in [34], define the Green–Taylor solutions to the NSE.

DEFINITION 3. *Let $\phi(x)$ be 2π-periodic and satisfy*

$$-\Delta\phi = \lambda\phi, \ \nabla\cdot\phi = 0.$$

Then the velocity-pressure pair (u,p) is a solution of the NSE, where

$$\begin{aligned} u(x,t) &= e^{-\nu\lambda t}\phi(x), \\ u\cdot\nabla u + \nabla p &= 0. \end{aligned} \tag{4.1}$$

It was shown in [50] that for such functions ϕ, $\nabla\times(\phi\cdot\nabla\phi) = 0$. Therefore, it follows from (4.1) that $\nabla\times(u\cdot\nabla u) = 0$ and such pressure exists.

We will need the fully continuous, strong formulations of the ADM, the ADC, and the filtered NSE for this benchmark problem ($f = 0$). The models seek to construct solution pairs (w_1,p_1) and (w_2,p_2) to approximate the true solution $(\bar{u},p)$.

$$\bar{u}_t - \delta^2\Delta\bar{u}_t - \nu\Delta\bar{u} + \nu\delta^2\Delta^2\bar{u} + (\bar{u}-\delta^2\Delta\bar{u})\cdot\nabla(\bar{u}-\delta^2\Delta\bar{u}) + \nabla p = 0, \tag{4.2}$$

$$w_{1,t} - \delta^2\Delta w_{1,t} - \nu\Delta w_1 + \nu\delta^2\Delta^2 w_1 + w_1\cdot\nabla w_1 + \nabla p_1 = 0, \tag{4.3}$$

$$\begin{aligned} &w_{2,t} - \delta^2\Delta w_{2,t} - \nu\Delta w_2 + \nu\delta^2\Delta^2 w_2 + w_2\cdot\nabla w_2 + \nabla p_2 \\ &\quad = -\delta^2 w_1\cdot\nabla(-\Delta w_1) - \delta^2(-\Delta w_1)\cdot\nabla w_1 - \delta^2(-\Delta w_1)\cdot\nabla(-\Delta w_1). \end{aligned} \tag{4.4}$$

When comparing the ADM versus the ADC, one should remember that both models aim to approximate the averaged velocity $\bar{u}$ and, depending on the setup, either the exact or the averaged pressure (p or $\bar{p}$). Thus, the consideration of the models (4.3)–(4.4) should start with the discussion on (4.2).

THEOREM 6. *A solution pair $(\bar{u},p)$ of (4.2) exists, where*

$$\begin{aligned} \bar{u}(x,t) &= e^{-\nu\lambda t}\phi(x), \\ (1+\lambda\delta^2)^2\bar{u}\cdot\nabla\bar{u} + \nabla p &= 0. \end{aligned} \tag{4.5}$$

Proof. The proof follows the proofs in [50] and [34]. The vector $\bar{u}\cdot\nabla\bar{u}$ is curl-free, therefore such pressure exists. It is also a simple exercise to verify that

$$\bar{u}_t - \delta^2\Delta\bar{u}_t - \nu\Delta\bar{u} + \nu\delta^2\Delta^2\bar{u} = 0. \qquad \square$$

The models (4.3)–(4.4) are analyzed in the same manner, leading to the next theorem.

THEOREM 7. *There exist solution pairs* (w_1, p_1) *of* (4.3) *and* (w_2, p_2) *of* (4.4)*, respectively, where*

$$w_1(x,t) = e^{-\nu\lambda t}\phi(x), \qquad w_1 \cdot \nabla w_1 + \nabla p_1 = 0, \tag{4.6}$$

and

$$w_2(x,t) = e^{-\nu\lambda t}\phi(x), \tag{4.7}$$

$$w_2 \cdot \nabla w_2 + \nabla(p_2 - ((1+\lambda\delta^2)^2 - 1)p_1) = 0.$$

Proof. The proof of (4.6) closely follows that of Theorem 6; the result of (4.6) is then used to show (4.7). ∎

On one hand, these results show that the ADC, just like the ADM, possesses an exact solution with exactly the same fundamental structure as the Taylor–Green solution of the NSE. However, there is more information that can be squeezed from Theorems 6–7. Compare the second equations of (4.5), (4.6), and (4.7):

$$\begin{aligned} \bar{u} \cdot \nabla \bar{u} + (2\lambda\delta^2 + \lambda^2\delta^4)\bar{u} \cdot \nabla \bar{u} + \nabla p &= 0, \\ w_1 \cdot \nabla w_1 + \nabla p_1 &= 0, \\ w_2 \cdot \nabla w_2 + (2\lambda\delta^2 + \lambda^2\delta^4) w_1 \cdot \nabla w_1 + \nabla p_2 &= 0. \end{aligned} \tag{4.8}$$

This comparison clearly shows how the ADC aims to superseed the ADM in approximating $(\bar{u}, p)$. Both models are comparable when computing the large scales (small values of λ). The ADC, however, goes one large step further than the ADM in trying to accurately model the small scales (large λ).

4.1. Accuracy and convergence rates. In this subsection we compare the ADC with two of its most natural competitors: the ADM (also called ADM_0 to indicate the choice $N = 0$ in Definition 1) given by (2.8) and the theoretically fourth order accurate (in δ) model ADM_1. The latter is created with the choice $N = 1$ in Definition 1 and requires d extra variables in R^d to approximate the double filter $\bar{\bar{w}}_1$. We will show that ADC outperforms both models on a problem with known true solution, and then demonstrate the clear advantage of the ADC in computing the drag and lift coefficients.

First, we consider the ADC for a problem with low viscosity, $\nu = 10^{-3}$, but known true solution. The second order accurate Crank–Nicolson method is used for time discretization, instead of the backward Euler. The true solution of the two-dimensional traveling wave test problem is given by

$$\begin{aligned} u_1 &= \frac{3}{4} + \frac{1}{4}\cos(2\pi(x-t))\sin(2\pi(y-t))e^{-8\pi^2 t\nu}, \\ u_2 &= \frac{3}{4} - \frac{1}{4}\sin(2\pi(x-t))\cos(2\pi(y-t))e^{-8\pi^2 t\nu}, \\ p &= \frac{-1}{64}(\cos(4\pi(x-t)) + \cos(4\pi(y-t)))e^{-16\pi^2 t\nu}. \end{aligned}$$

The right-hand side was computed to match the true solution above; the domain was the unit square, with N mesh nodes per side; the final time was $T = 1$.

The expected accuracy of the model is $O(\delta^4 + \Delta t^2 + h^k)$, when a pair of piecewise polynomials (P_k, P_{k-1}) is used for finite element velocity-pressure spaces. Thus, in

order to achieve overall second order accuracy, one would need to employ the (P_4, P_3) finite elements, along with the time step $\Delta t = h^2$. Performing enough mesh refinements to capture the asymptotic convergence of the ADC to fourth order accuracy would be too computationally expensive—exactly as claimed by those who do not believe that a defect correction idea could be fruitful in CFD. However, Tables 1–3 demonstrate that, even if fourth order accuracy is not achieved, the ADC still outperforms both ADM_0 and ADM_1.

With the choice $\Delta t = h = \delta$ we can only expect second order accuracy from both the ADM and the ADC.

Table 1 shows that the error in the ADC approximation is roughly twice as small as the error in the ADM. Thus, in order for the ADM to perform with the same accuracy as the ADC, it would require a mesh refinement of $h_{new} = \frac{h_{old}}{\sqrt{2}}$. With the increased size of the ADM system and the increased number of time steps, one would need to triple the computational time needed for the ADM to achieve the accuracy of the ADC. Meanwhile, with the natural parallel implementation, the ADC only takes about 40% extra time, compared to the ADM on the same mesh.

It took approximately 30 hours for the ADC to obtain the results in the last row of Table 1. It would have taken the ADM more than 60 hours to get the same accuracy (or worse, considering all the complications that can arise with mesh refinement in turbulence modeling). The situation is even worse for the ADM_1 model. Applied to the same problem, it gave worse results than both the ADM and ADC, while requiring substantially more computational time (37 hours for the case $N = 64$). Inaccuracy of ADM_1 can be attributed to the problem setting, where fourth order accuracy cannot be achieved; further investigation is needed for more in-depth comparison of ADM_1 versus the ADC. Also, all of the above models would benefit from a good choice of a preconditioner (no preconditioners used in the above computations), which is yet another topic for future investigation.

Tables 2–3 provide another way of showing the higher order accuracy of the ADC with respect to the filtering width. When both the mesh diameter and the time step are fixed, and the filtering width is refined, we clearly see the ADC outperform the ADM. Eventually, as the filtering width becomes less than the mesh diameter, the spatial and temporal discretization errors start to outweigh the modeling error, and the convergence rates of the ADC decline to second order.

TABLE 1
ADM (w_1) versus ADC (w_2), $\nu = 0.001, h = \Delta t = \delta$.

N	$\|\| \bar{u} - w_1 \|\|_{L^2(0,T;L^2(\Omega))}$	$\|\| \bar{u} - w_2 \|\|_{L^2(0,T;L^2(\Omega))}$	$\|\| \bar{u} - w_1^h \|\|_{L^2(0,T;H^1(\Omega))}$	$\|\| \bar{u} - w_2^h \|\|_{L^2(0,T;H^1(\Omega))}$
8	0.00523349	0.00508257	0.0726956	0.0762683
16	0.00180541	0.00131433	0.0251442	0.0203907
32	0.000526616	0.000290644	0.00723852	0.00429708
64	0.000136304	6.96E-05	0.00186818	0.00101774

TABLE 2
ADM (w_1) versus ADC (w_2), $\nu = 0.001, h = \Delta t = \frac{1}{64}$.

$\frac{1}{\delta}$	$\|\| \bar{u} - w_1 \|\|_{L^2(0,T;L^2(\Omega))}$	$\|\| \bar{u} - w_2 \|\|_{L^2(0,T;L^2(\Omega))}$	$\|\| \bar{u} - w_1^h \|\|_{L^2(0,T;H^1(\Omega))}$	$\|\| \bar{u} - w_2^h \|\|_{L^2(0,T;H^1(\Omega))}$
16	0.0079828	0.0105843	0.1511	0.234986
32	0.00339996	0.00361988	0.0742057	0.126106
64	0.00104965	0.000685599	0.0281213	0.0310733
128	0.000298603	0.000160771	0.00950088	0.00617638

TABLE 3
Convergence rates for errors from Table 2.

$\frac{1}{\delta}$	Rate of w1 in $L^2(L^2)$	Rate of w2 in $L^2(L^2)$
16	-	-
32	1.23	1.55
64	1.69	2.4
128	1.81	2.1

The above test demonstrates the ability of the ADC to outperform its competitors and achieve the needed accuracy faster than the ADM, for a manufactured test problem.

4.2. Drag and lift coefficients. Next we apply the proposed method to a well-known benchmark problem of computing the drag and lift coefficients. Note that this problem is mostly used for turbulence models that seek to approximate the true velocity u, whereas the ADM approximated $\bar{u}$. This makes this test problem all the more challenging—and therefore interesting—as we will report the exact deconvolution of the computed solutions, $(I - \delta^2\Delta)w_1$ and $(I - \delta^2\Delta)w_2$, and compare them against the available reference data for the true solution u (not $\bar{u}$).

Following [26, 48, 49], we consider the two-dimensional flow in $\Omega = [0, 2.2] \times [0, 0.41]$ past the cylinder of base radius 0.05, centered at $(0.15, 0.15)$. Take $f = 0$, $\nu = 0.001$, final time $T = 8$. For the left-to-right flow prescribe the inflow and outflow profile

$$\mathbf{u}(t; 0, y) = \mathbf{u}(t; 2.2, y) = \frac{1}{0.41^2} \sin(\pi t/8)(6y(0.41 - y), 0).$$

No-slip conditions are prescribed at the other boundaries. The drag and lift coefficients $c_d(t)$ and $c_l(t)$ are computed with both the ADM and the ADC, and the maximal values of these coefficients are compared against the reference values in [26]. The number of degrees of freedom is 22,204 for velocity and 5,663 for pressure (compared to 25,408 and 3,248 in [26], level 2).

The results are presented in Tables 4–5 and provide a compelling evidence of high physical fidelity of the proposed ADC model.

The drag coefficients were computed at $\delta = 0.5h$, and one extra refinement of the filtering width was needed to capture the lift coefficients, $\delta = 0.25h$.

The ADC approximates the maximal drag and lift coefficients at least 10 times more accurately than the ADM! Also, just as described in [26], the lift coefficient is more "sensitive" than the drag coefficient, and it requires a smaller filtering width.

TABLE 4
Maximal drag and lift coefficients, $\Delta t = 0.04$, $h = 1/64$.

-	Reference value	Value, computed by the ADM	Value, computed by the ADC	
Drag	2.9507820	2.96532	2.94932	
Lift	0.46134147	0.354731	0.463541	

TABLE 5
Errors in drag-lift coefficient computations, ADM versus ADC.

-	|ADM error|	|ADC error|
Drag	0.014538	0.001462
Lift	0.10661047	0.00219953

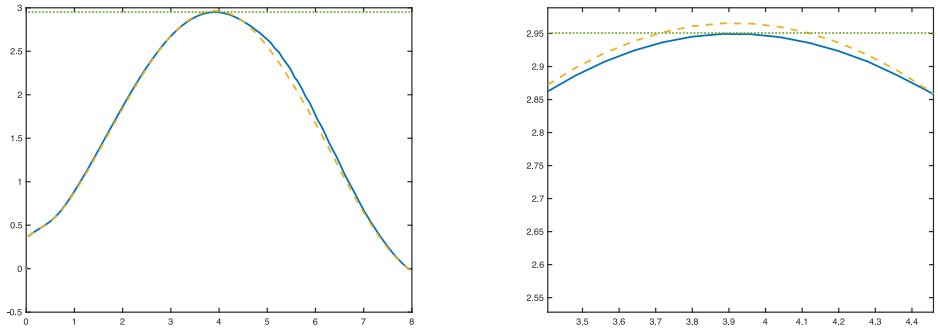

(a) Drag coefficients computed by the ADM and ADC, $\delta = \frac{h}{2}$

(b) Drag coefficients, zoomed in near $t = 4$

FIG. 1. *Drag coefficients computed by the ADM (dashed line) and ADC (solid line),* $\delta = \frac{h}{2}$. *Reference value is shown as the dotted horizontal line.*

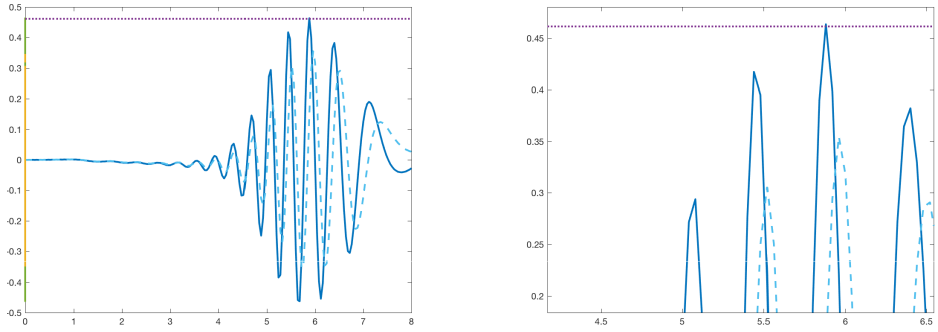

(a) Lift coefficients computed by the ADM and ADC, $\delta = \frac{h}{4}$

(b) Lift coefficients, zoomed in near $t = 6$

FIG. 2. *Lift coefficients computed by the ADM (dashed line) and ADC (solid line),* $\delta = \frac{h}{4}$. *Reference value is shown as the dotted horizontal line.*

Next we present the plots of the models' drag and lift coefficients, computed as functions of time, $0 \leq t \leq 8$. These are to be compared with the corresponding plots in [26, 49].

Given that the chosen benchmark problem is not ideally suited for the ADC, it would be very interesting to create and apply other LES-C models to this benchmark problem and compare them with the performance of the respective underlying LES models.

4.3. Flow past the step. For the last qualitative test, we use both the ADM and the ADC to model the flow past a forward-backward facing step. This is a well-studied benchmark problem (see, e.g., [22, 27, 37, 38]), where, at a certain range of the Reynolds number, the true solution is still computationally feasible and yet it possesses interesting qualitative features that should be captured by a good turbulence model. Namely, for $500 \leq Re \leq 700$ a recirculation region is clearly seen behind the step, where vortices are formed; with time, they shed, deform, and travel with the flow. If a model's solution possesses all these features, but shows signs of retardation

(be that the retardation of the shedding or the slower propagation of the vortices), it is usually regarded as a sign that the model is too dissipative. This has been reported in regard to the ADM, and we want to see how the ADC would perform in this setting.

Following the setting of, e.g., [37], we consider the domain $[0, 40] \times [0, 10]$ with the step of unit height at $5 \leq x \leq 6$. For both model solutions w_1 and w_2 we impose the parabolic inflow and outflow boundary conditions $u_i = y(10 - y)/25, v_i = 0$, where $w_i = (u_i, v_i)^T$, $i = 1, 2$. No-slip boundary conditions are imposed on the rest of the boundary.

The aim of this test is twofold. First, we want to show that both the ADM and, more importantly, the ADC can capture the behavior of the averaged true solution, while using a much coarser mesh. Second, on that coarse mesh, we will show that the ADC better captures the qualitative behavior of the averaged true solution than the ADM. Figures 3, 4, and 5 show the plots of the true solution (fine mesh) and the models' solutions (coarse mesh, less than a third of the total number of degrees of freedom, compared to the fine mesh) at time $T = 40$. All computations were performed with the time step $\Delta t = 0.01$; the filtering width in both ADM and ADC was chosen to be $\delta = 0.125$. Both the ADM and the ADC correctly capture the shedding (three vortices are clearly seen in all three plots). However, the ADM incorrectly predicts the speed with which the first vortex is traveling with the flow; this hints at the ADM being too dissipative (which is agreed upon by many researchers, and motivates extra investigation, like the ADM with time relaxation). At the same time, the ADC is able to correctly predict the speed of all eddies—even on a much coarser mesh.

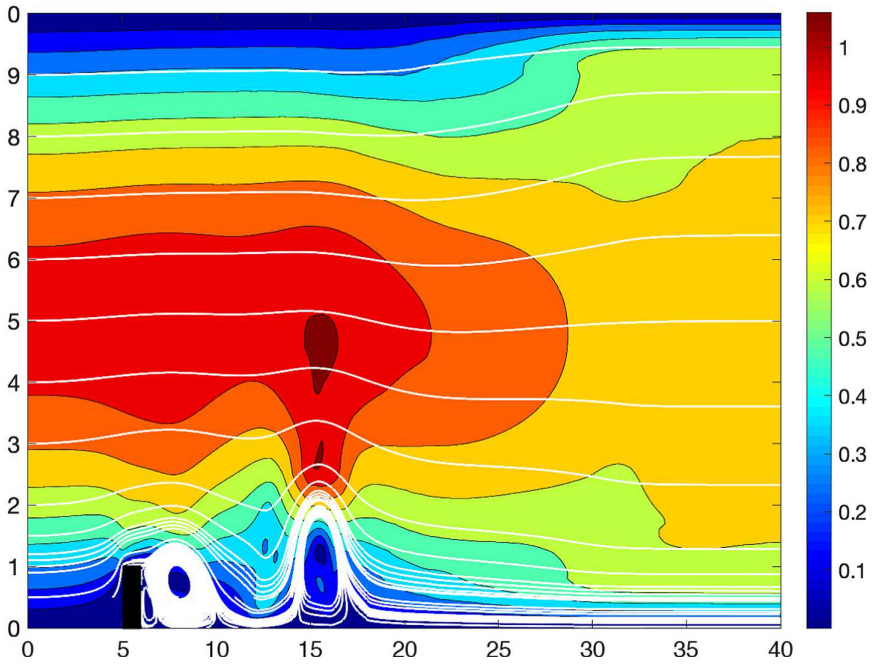

FIG. 3. *Filtered true velocity,* $Ndofs = 33{,}820$.

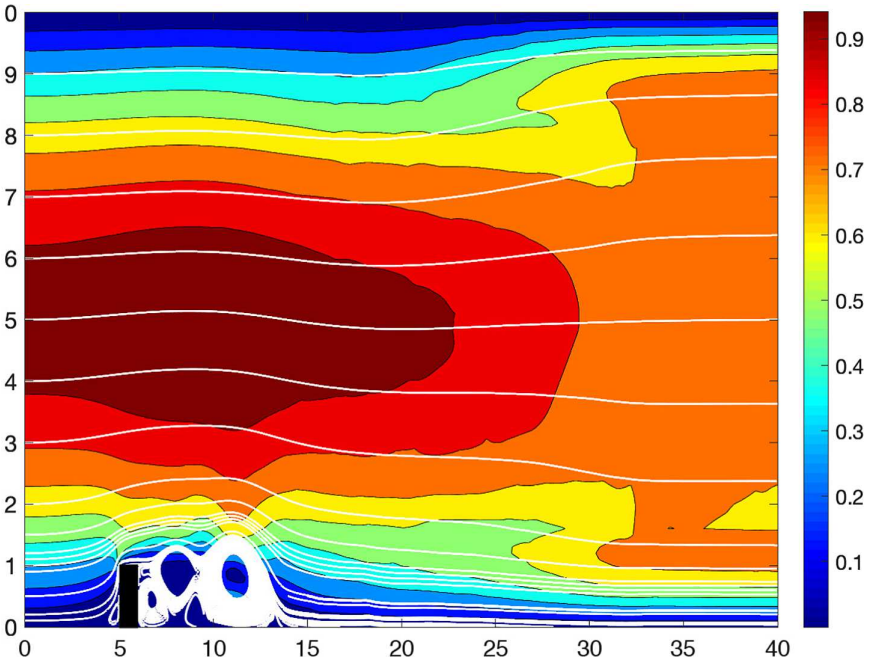

FIG. 4. *ADM solution, $Ndofs = 8897$.*

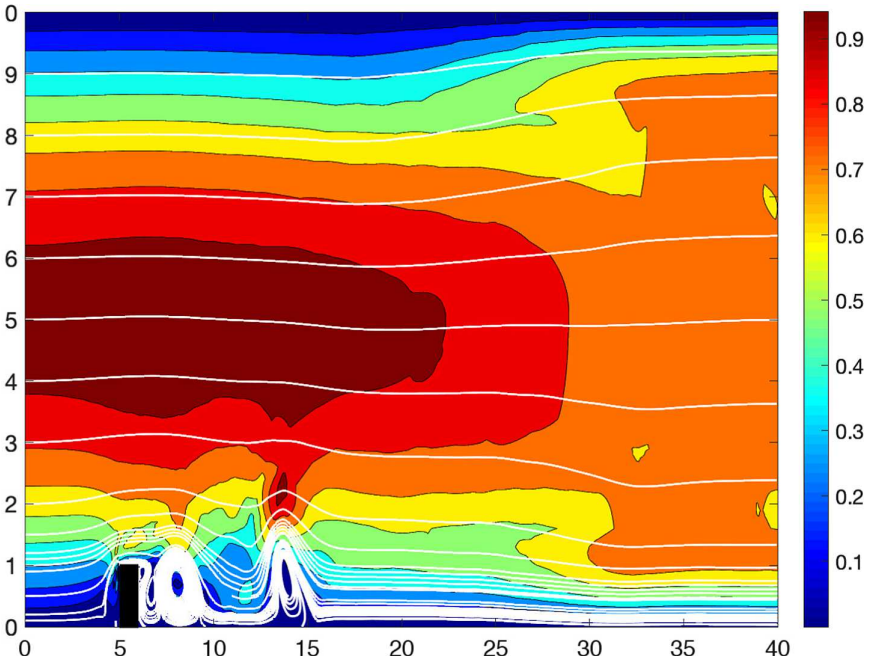

FIG. 5. *ADC solution, $Ndofs = 8897$.*

5. Conclusion. We introduced a new family of models for high Reynolds number flows, LES-C, that combines a LES approach to turbulence modeling with a defect correction methodology. One of these models, based on the ADM, was investigated

both numerically and theoretically. The model, ADC, was shown to be stable and higher order accurate with respect to the filtering width. It was compared against its most natural competitor, the ADM, when applied to a problem with known solution. The ADC outperformed the ADM in terms of accuracy per computational time: in order to achieve the prescribed tolerance, it would have taken the ADM more than twice the time needed for the ADC. Just like the ADM, the ADC was shown to possess an exact solution to the Green–Taylor vortex problem; this analytical solution also demonstrated the way in which the ADC builds a better approximation to the averaged true velocity than the ADM.

The ADC solution did not achieve the claimed fourth order accuracy in the filtering width δ, and the author attributes this to the well-known asymptotic convergence of defect correction methods. In order to see the higher order accuracy, one would need to keep refining δ. But, since the other two components of the overall error were not improved by the ADC, it would have taken prohibitively small time steps and mesh diameters to reach the claimed rates.

The ADC was also tested on a benchmark problem of computing drag and lift coefficients past a two-dimensional circular obstacle. The results were at least 10 times more accurate than those obtained by the ADM!

Finally, the ADC and ADM models were also compared when modeling a flow past the step. The ADM was shown to be too dissipative, while the ADC was able to correctly predict the speed with which the eddies were propagating—even on a coarse spatial mesh.

REFERENCES

[1] M. Aggul, J. Connors, D. Erkmen, and A. Labovsky, *A defect-deferred correction method for fluid-fluid interaction*, SIAM J. Numer. Anal., 56 (2018), pp. 2484–2512.

[2] M. Aggul, F. Eroglu, S. Kaya, and A. Labovsky, *A projection based variational multiscale method for atmosphere-ocean interaction*, Comput. Methods Appl. Mech. Engrg., 365 (2020), 112957.

[3] M. Aggul, S. Kaya, and A. Labovsky, *Two approaches to creating a turbulence model with increased temporal accuracy*, Appl. Math. Comput., 358 (2019), pp. 25–36.

[4] M. Aggul and A. Labovsky, *A high accuracy minimally invasive regularization technique for Navier-Stokes equations at high Reynolds number*, Numer. Methods Partial Differential Equations, 33 (2017), pp. 814–839.

[5] U. M. Ascher, S. J. Ruuth, and B. T. R. Wetton, *Implicit-explicit methods for time-dependent partial differential equations*, SIAM J. Numer. Anal. 32 (1995), pp. 797–823.

[6] J.-W. Bao, J. M. Wilczak, J.-K. Choi, and L. H. Kantha, *Numerical simulations of air-sea interaction under high wind conditions using a coupled model: A study of hurricane development*, Monthly Weather Rev., 128 (2000), pp. 2190–2210.

[7] C. Bernardi, T. Chacon-Rebello, M. Gomez, R. Lewandowski, and F. Murat, *A model of two coupled turbulent fluids, Part* II*: Numerical approximations by spectral discretization*, SIAM J. Numer. Anal., 40 (2002), pp. 2368–2394.

[8] L. C. Berselli, *On the Large Eddy Simulation of the Taylor-Green vortex*, J. Math. Fluid Mech., 7 (2005), pp. 164–191.

[9] L. Berselli, T.-Y. Kim, and L. Rebholz, *Analysis of a reduced-order approximate deconvolution model and its interpretation as a Navier-Stokes-Voigt regularization*, Discrete Contin. Dyn. Syst. Ser. B, 21 (2016), pp. 1027–1050.

[10] K. Böhmer, P. W. Hemker, and H. J. Stetter, *The defect correction approach*, in Defect Correction Methods: Theory and Applications, K. Böhmer, and H. J. Stetter, eds., Springer Verlag, Berlin, 1984, pp. 1–32.

[11] A. Bourlioux, A. T. Layton, and M. L. Minion, *High-order multi-implicit spectral deferred correction methods for problems of reactive flows*, J. Comput. Phys., 189 (2003), pp. 651–675.

[12] D. Bresch and J. Koko, *Operator-splitting and Lagrange multiplier domain decomposition methods for numerical simulation of two coupled Navier-Stokes fluids*, Int. J. Appl. Math. Comput. Sci., 16 (2006), 2006, pp. 419–429.

[13] F. O. Bryan, B. G. Kauffman, W. G. Large, and P. R. Gent, *The NCAR CESM Flux Coupler*, Tech. Report NCAR/TN-424+STR, National Center for Atmosphere Research, 1996.

[14] E. Burman, and M. A. Fernández, *Stabilization of explicit coupling in fluid-structure interaction involving fluid incompressibility*, Comput. Methods Appl. Mech. Engrg., 198 (2009), pp. 766–784.

[15] J. Connors, J. Howell, and W. Layton, *Decoupled time stepping methods for fluid-fluid interaction*, SIAM J. Numer. Anal., 50 (2012), pp. 1297–1319.

[16] A. Dunca and Y. Epshteyn, *On the Stolz–Adams deconvolution model for the large eddy simulation of turbulent flows*, SIAM J. Math. Anal., 37 (2006), pp. 1890–1902.

[17] A. Dutt, L. Greengard, and V. Rokhlin, *Spectral deferred correction methods for ordinary differential equations*, BIT, 40 (2000), pp. 241–266.

[18] D. Erkmen and A. Labovsky, *Defect-deferred correction method for the two-domain convection-dominated convection-diffusion problem*, J. Math. Anal. Appl., 450 (2017), pp. 180–196.

[19] V. J. Ervin and H. K. Lee, *Defect correction method for viscoelastic fluid flows at high Weissenberg number*, Numer. Methods Partial Differential Equations, 22 (2006), pp. 145–164.

[20] G. P. Galdi, *An Introduction to the Mathematical Theory of the Navier-Stokes Equations Volume* I*: Linearized Stedy Problems*, Springer Tracts Natural Philosophy 38, Springer-Verlag, New York, 1994.

[21] V. Girault and P. A. Raviart, *Finite Element Approximation of the Navier-Stokes Equations*, Lecture Notes in Math., 749, Springer-Verlag, New York, 1979.

[22] M. D. Gunzburger, *Finite Element Methods for Viscous Incompressible Flows: A Guide to Theory, Practices, and Algorithms*, Academic Press, New York, 1989.

[23] M. Gunzburger and A. Labovsky, *High accuracy method for turbulent flow problems*, Math. Models Methods Appl. Sci., 22 (2012).

[24] F. Hecht, A. LeHyaric, and O. Pironneau, *Freefem++ Version* 2.24-1, http://www.freefem.org/ff++, 2008.

[25] J. G. Heywood and R. Rannacher, *Finite-elements approximation of the nonstationary Navier-Stokes problem. Part* IV*: Error analysis for second-order discretization*, SIAM J. Numer. Anal., 27 (1990), pp. 353–384.

[26] V. John, *Reference values for drag and lift of a two-dimensional time-dependent flow around a cylinder*, Numer. Methods Fluids, 44 (2004), pp. 777–788.

[27] V. John and A. Liakos, *Time dependent flow across a step: the slip with friction boundary condition*, Internat. J. Numer. Methods. Fluids, 50 (2006), pp. 713–731.

[28] A. Labovsky, *A defect correction approach to turbulence modeling*, Numer. Methods Partial Differential Equations, 31 (2015), pp. 268–288.

[29] A. Labovsky, *A defect correction method for the evolutionary convection diffusion problem with increased time accuracy*, Comput. Methods Appl. Math., 9 (2009), pp. 154–164.

[30] A. Labovsky, *A defect correction method for the time-dependent Navier-Stokes equations*, Numer. Methods Partial Differential Equations, 25 (2008), pp. 1–25.

[31] A. Labovsky and C. Trenchea, *A family of approximate deconvolution models for magnetohydrodynamic turbulence*, Numer. Funct. Anal. Optim., 31 (2010), pp. 1362–1385.

[32] A. Labovsky and C. Trenchea, *Large eddy simulation for turbulent magnetohydrodynamic flows*, J. Math. Anal. Appl., 377 (2011), pp. 516–533.

[33] A. Labovsky, C. Trenchea, and N. Wilson, *High accuracy method for magnetohydrodynamics system in Elsasser variables*, Comput. Methods Appl. Math., 15 (2015), pp. 97–110.

[34] W. Layton, *On Taylor/Eddy solutions of approximate deconvolution models of turbulence*, Appl. Math. Lett., 24 (2011), pp. 23–26.

[35] W. Layton, H. K. Lee, and J. Peterson, *A defect-correction method for the incompressible Navier–Stokes equations*, Appl. Math. Comput., 129 (2002), pp. 1–19.

[36] W. Layton and R. Lewandowski, *A high accuracy Leray-deconvolution model of turbulence and its limiting behavior*, Anal. Appl., 6 (2008), pp. 23–49.

[37] W. Layton, C. Manica, M. Neda, and L. Rebholz, *Numerical analysis of a high accuracy Leray-deconvolution model of turbulence*, Numer. Methods Partial Differential Equations, 24 (2008), pp. 555–582.

[38] W. Layton and L. Rebholz, *Approximate Deconvolution Models of Turbulence: Analysis, Phenomenology and Numerical Analysis*, Lecture Notes in Math. 2042, Springer-Verlag, Berlin, 2016.
[39] F. Lemarie, E. Blayo, and L. Debreu, *Analysis of ocean-atmosphere coupling algorithms: Consistency and stability*, Procedia Comput. Sci., 51 (2015), pp. 2066–2075.
[40] J.-L. Lions, R. Temam, and S. Wang, *Models of the coupled atmosphere and ocean (CAO* I*)*, Comput. Mech. Adv., 1 (1993), pp. 5–54.
[41] J.-L. Lions, R. Temam, and S. Wang, *Models of the coupled atmosphere and ocean (CAO* II*)*, Comput. Mech. Adv., 1 (1993), pp. 55–119.
[42] J. Mathew, *Large eddy simulation of a premixed flame with approximate deconvolution modeling*, Proc. Combustion Institute, 29 (2002), pp. 1995–2000.
[43] M. L. Minion, *Semi-implicit spectral deferred correction methods for ordinary differential equations*, Comm. Math. Sci. 1 (2003), pp. 471–500.
[44] M. L. Minion, *Semi-implicit projection methods for incompressible flow based on spectral deferred corrections*, Appl. Numer. Math., 48 (2004), pp. 369–387.
[45] N. Perlin, E. D. Skyllingstad, R. M. Samelson, and P. L. Barbour, *Numerical simulation of air-sea coupling during coastal upwelling*, J. Phys. Oceanography, 37 (2007), pp. 2081–2093.
[46] C. Ross Ethier and D. A. Steinman, *Exact fully 3D Navier-Stokes solutions for benchmarking*, Internat. J. Numer. Methods Fluids, 19 (1994), pp. 369–375.
[47] S. Stolz and N. A. Adams, *An approximate deconvolution procedure for large-eddy simulation*, Physics of Fluids, 11 (1999).
[48] V. John and J. Rang, *Adaptive time step control for the incompressible Navier-Stokes equations*, Comput. Methods Appl. Mech. Engrg. 199 (2010), pp. 514–524
[49] V. John, *Finite Element Methods for Incompressible Flow Problems*, Springer Ser. Comput. Math. 51, Springer, Verlag, Berlin, 2016.
[50] O. Walsh, *Eddy solutions of the Navier-Stokes equations*, in *The NSE* II*: Theory and Numerical Methods*, J. G. Heywood, K. Masuda, R. Rautmann, V. A. Solonnikov, eds., Lecture Notes in Math. 1530, Springer-Verlag, Berlin, 1992.
[51] X. Xie, D. Wells, Z. Wang, and T. Iliescu, *Approximate deconvolution reduced order modeling*, Comput. Methods Appl. Mech. Engrg., 313 (2017), pp. 512–534.